

# COMPUTATIONAL MODEL FOR PROBABILITY PREDICTION OF SCAN PATHS IN STATIC SCENES

Yorie Nakahira<sup>1</sup> and Nakayama Minoru<sup>2</sup>

<sup>1</sup>Control and Systems Engineering, Tokyo Institute of Technology, Tokyo, Japan

<sup>2</sup>Department of Human System Science, Tokyo Institute of Technology, Tokyo, Japan

Keywords: Eye Movements, Scan Path, Fixation, Static Scenes, Probability Prediction.

Abstract: We develop a computational model of scan paths when viewing static images. The proposed scan path model generates a dynamic distribution of visual attention using multiple image processing algorithms based on biological principles. The probability of any scan paths is computed from this distribution of visual attention at each subsequent numbered fixation. The validity of our model is tested using eye movement data. Our results verify the possibility of conventionally infeasible modeling of the scan paths for static images.

## 1 INTRODUCTION

Despite the promise of scan path prediction (Robert et al., 2003), a two-fold scan path prediction problem exists for static images. First, scan paths are rarely coherent from person to person (Bohme et al., 2004). The possible accuracy of any conventional model which outputs a single probable scan path cannot exceed the low coincidence level of scan paths from different viewers (Privitera and Stark, 2000). In addition, for the purpose of usability evaluation, it is unreasonable to ignore many other possible scan paths merely because they are not the most probable ones. Second, processing an image using an algorithm can only yield static parameters for visual conspicuousness, whereas temporal eye movements are dynamic and so are their distribution. Therefore estimating dynamic change using static parameters is self-limiting.

This paper suggests a novel way for scan path prediction that is based on two premises; (1) a scan path prediction model should yield the possibility (distribution) of visual attention and scan paths instead of the most probable scan path; (2) that the model should incorporate several algorithms for eye movement prediction to optimize its value over the temporal sequence of fixations (subsequent numbered fixations).

By assuming the computability of the statistical distribution of scan paths, we compute the distribution of visual attention along the temporal sequence of fixations. In this way, variations in personal visual behavior can be suitably expressed through statisti-

cal expression, instead of as aberrations. The computation of the distribution of visual attention is quite useful, as it makes a previously *impossible* prediction possible for scan paths when static images are viewed. A model of scan path prediction is proposed in Section 2. Section 3 describes the experimental protocol to acquire eye movement data. Section 4 presents the experimental results. Section 5 summarize the study presented here.

## 2 PROPOSED MODEL

### 2.1 Attention Distribution Prediction

The displayed image was first labeled according to each region of interest. Take figure 1 for example. The pie-graph represents a data set with three components, each labeled from 1 to 3. Conditions excluding the above-mentioned state 1 to 3 are brief enough so that they can be categorized as intervals during which the state of visual attention changes.

Attention Distribution Ratio (ADR) is defined as the ratio of attention to each position on the image. Each pixel value of an image is labeled from 1 to  $z$ . The number of labels,  $z$ , is determined by the number of objects in the image, or the number of positions which represent different meanings. If the ratio of subjects that fixate at labels 1, 2 and 3 are 1 : 2 : 1 (experimental ADR), the ideal computational algorithms for computed ADR are expected to generate a value

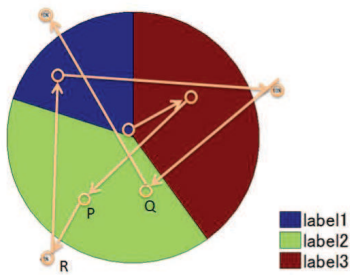


Figure 1: Example of a scan path and its labeling. Each pixel value of the image is labeled from 1 to 3. The cases when a subject fixates at the positions labeled 1, 2, 3 are defined as state 1, state 2, and state 3 respectively. The scan path noted in this figure, for example, is "1 → 3 → 2 → 2 → 1 → 3 → 2 → 1".

close to "state1 : state2 : state3 = 1 : 2 : 1".

This algorithmically computed ADR is calculated using the following three procedures.

- I. Converting a image (static visual environment) into maps using image processing algorithms (IPAs) whose pixel values denote the visual conspicuousness, in other words the likelihood to be viewed. Suggested IPAs are defined in Section 3.3.
- II. Each pixel value of the map is labeled from 1 to  $z$  according to the meaning it represents.  $z$  is the number of objects in the image. This labeling simplifies the large image size into a small number of sections and makes the computational procedure less demanding. For the experiments in this study, an example of labeling is explained in Section 5.1.1.
- III. The visual conspicuousness represented by the pixel value is summed up separately for each labeled region. The ratio of the summation values of differently labeled regions is expected to denote the relative amounts of visual attention each region is likely to receive. This quantitatively expressed likelihood to be viewed is defined as cADR (computed Attention Distribution Ratio).

An important thing to note is that conventional models usually only have procedure I, and produce an output of only a single scan path. However, procedures II and III are significant because these are steps that afford the model to take the personal difference of the scan paths into consideration.

## 2.2 Computing Scan Path Probability

Since the distribution of visual attention changes over time, it is unreasonable to expect a single IPA to yield accurate prediction results over temporal number of

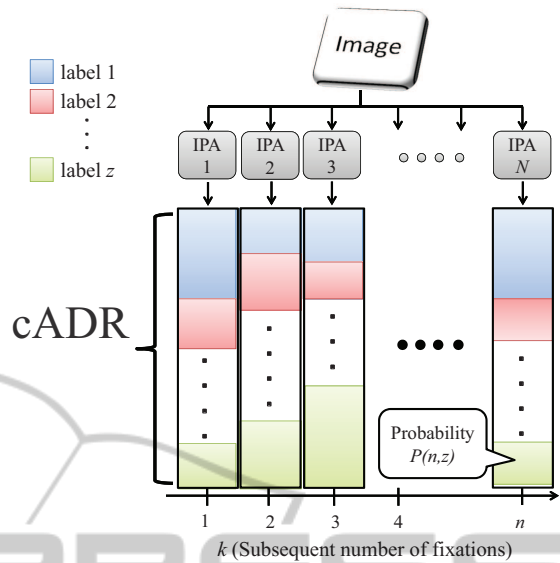


Figure 2: Computation of cADR to predict scan paths when viewing a static image. First, the image is processed using IPAs to yield cADR for each subsequent numbered fixation that indicate the possibility of being state  $s$  ( $s \in 1, \dots, z$ ). The resultant cADR indicates the statistical distribution of state  $s$  at  $k$ th fixation ( $k = 1, \dots, n$ ) (section 3.1).  $P(n, z)$  is defined to be the probability of state  $z$  at the  $n$ th fixation. The probability of the scan path " $s_1, \dots, s_n$ " can then be calculated as  $P(1, s_1) \dots P(n, s_n)$  (section 3.2).

fixations. Consequently, our model optimizes itself over time; in other words, over the subsequent numbered fixations. This optimization is achieved by using IPAs in a manner where each IPA is used only when it is at highest accuracy.

The overview of our model for computing cADR from a set of IPAs throughout the subsequent numbered fixations is defined in figure 2.  $P(k, s)$  is defined to be the computed probability of eye movement at state  $s$  (subjects fixating at the position labeled  $s$ ) at  $k$ th fixation. The  $P(k, s)$  is computed for  $k$ th fixation ( $k = 1, \dots, n$ ) from the IPA that are most suitable for the  $k$ th fixation. The biological principles represented by IPAs include the intuitive tendencies of eye movement such as fixating at the centers of images, fixating at the salient positions, and the task-oriented cognitive model. The choice IPAs for each subsequent numbered fixation is constructed on a case by case basis depending on the context under which viewers are put. The possibility of the scan path "state :  $s_1 \rightarrow s_2 \rightarrow s_3 \rightarrow \dots \rightarrow s_n$ " is computed as

$$P(1, s_1) \cdot P(2, s_2) \cdot P(3, s_3) \cdot \dots \cdot P(n, s_n) \quad (1)$$

We used the following algorithms (IPAs) in the new model;  $C$ : center-surround map, and  $D$ : Attention Distribution Map, and  $S$ : Saliency map (Iit et al., 1998). All three IPAs are based on the bottom-up im-

age based intuitive cognitive process or task-oriented attention element.

**C:** A Center-Surround map was generated by dropping an Gaussian kernel at the center of an image. The half-height width for the Gaussian is determined according to the area over which fixation can be said to exist. The biological background for the algorithms is based on the central fixation bias noted by previous studies (Buswell, 1935; Tatler, 2007).

**D:** An Attention Distribution Map combines the saliency map from Itti's model and a task relevance map. For Itti's model, the three conspicuity maps are normalized and summed together at an equal ratio, to become a saliency map ( $S$ ). For the task relevance map, under the context of the images being graphs, the quantitative data it represents is used as task-relevance. For each section labeled differently, the comparative amount representing each different region is used in a manner so that the larger the data, the higher the conspicuous value, the larger the cADR assigned to the region.

### 3 EXPERIMENTAL METHOD

During the experiment, eye movements were measured using an eye tracker (nac: EMR-NL, 640x460 pixel resolution, 60Hz). Images of graphs were displayed on a computer screen for three seconds each, followed by a one-second interval during which subjects fixate on a central cross. The coordinated positions on the images where subjects were looking was recorded for later analysis. The subjects were seated in front of a screen with their head secured to a chin-rest structure. The viewing distance was approximately 65 cm; the stimulus size was about 20 cm x 25 cm. In this paper, fixation is defined as a stable eye position with a velocity below the threshold of 20 degrees per second (Robert et al., 2003), and a scan path as the spatial arrangement of a sequence of fixations.

45 different images of graphs were utilized. There were five types of graphs with different design: two types of bar graphs and three types of pie charts. For each type of graph's design, there were 9 graphs representing 9 different sets of data. These 9 sets each have three components. Six subjects (3 male, 3 female) were used. Each subject repeated this experiments for 3 times.

## 4 RESULTS

### 4.1 Selection of IPAs for Each Subsequent Numbered Fixation

The best IPAs for each subsequent numbered fixation in the experimental situation are determined from the strength of the correlational relationship between eADR (experimental Attention Distribution Ratio) and cADR (computed Attention Distribution Ratio) from the 1st fixation to the 7th fixation. The cADR in the regions labeled from 1 to 3 by the method in section 5.1.1 are calculated for all images (45 images x 3 IPAs). The experimental Attention Distribution Ratio (eADR) of each subsequent numbered fixation on each image in the three second experiment was calculated. Then, the correlation coefficients between the computational data (cADR) and the experimental data (eADR) are computed from the 1st fixation to the 7th fixation.

Figure 3 plots the dynamic changes in correlational value (prediction accuracy) of IPAs from 1st fixation to the 7th fixation. The figure 3 confirms the expectation that each IPA has its own peak at a different subsequent numbered fixations. This data implies that the distribution of the scan path can be modeled by  $C$  from the 1st to the 2nd fixation, and by  $D$  from the 3rd to the 5th. In this way, the dynamic changes in the eADR over fixation number are suitably incorporated in the model by the shift of the static cADR computed by each IPA. The effectiveness of this is apparent when correlation values are compared with existing prediction model ( $S$ ), which defines an absolute single path by a single cADR.

The cADR computed from the above-mentioned model changes its value over the sequence of fixations by shifting the IPA. Thus, the model for ADR prediction can be defined as follows: IPA  $C$  calculate  $P(k, s)$  for  $k = 1, 2$ ; IPA  $D$  calculate  $P(k, s)$  for  $k = 3, 4$ . The calculation of the scan path probability is by equation 1.

### 4.2 Accuracy of the Model

Table 1 compares the probability of the computationally predicted scan paths (see equation 1) and the experimental probability when subjects are viewing a particular image. There are 81 ( $3^4$ ) possible states in total for the subsequent numbered fixations from 1 to 4, The table shows 4 types of scan paths with the highest computational probabilities. This result is encouraging because it suggests the validity of our proposed method of predicting possibility of scan paths.

The predicted probability of each scan path and

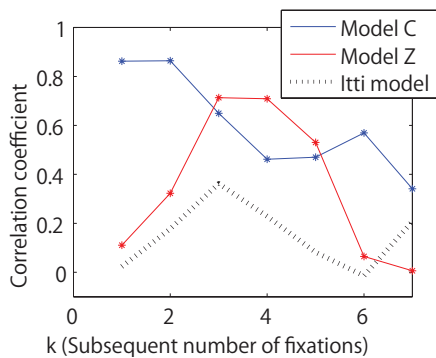


Figure 3: Changes in accuracy over the subsequent numbered fixations. This figure plots the correlational coefficient between eADR and the cADR computed from IPA C, D, or S on the y-axis, and the subsequent numbered fixations on the x axis. This figure implies that cADR can be optimized by predicting 1st to the 2nd fixations by C, 3rd to the 5th fixations by D.

Table 1: Computationally predicted scan paths and their experimental counterparts. This table compares the algorithmically computed scan paths probability with its experimental value.

Scan path	Computed	Experimental
2-3-1-1	0.335	0.389
2-2-3-2	0.166	0.056
2-2-2-3	0.166	0.167
2-2-2-2	0.082	0.111

the experimental probability of the scan path is compared using the correlational coefficient. Although 45 images, the correlational values is above 0.6 in 25 types of images, and above 0.4 in 35 types of images.

We also used the correlational coefficients between cADR and eADR as the index for the accuracy of the computational prediction. The high correlation between cADR and eADR means that the computationally predicted scan path probability could yield an accurate output.

Figure 4 plots the correlational value between cADR and eADR on the x axis and the variance of cADR on y axis. It is suggested from figure 4 that images with a high variance of cADR are generally predicted accurately, while images with low variance of cADR may not be reliably predicted. The biological meaning of the variation in cADR is that visual attention is likely to focus on a couple of labeled regions, rather than all of the existing regions. Therefore, variances in cADR values can be the index for model accuracy.

## 5 SUMMARY

In summary, this paper proposed a novel method of

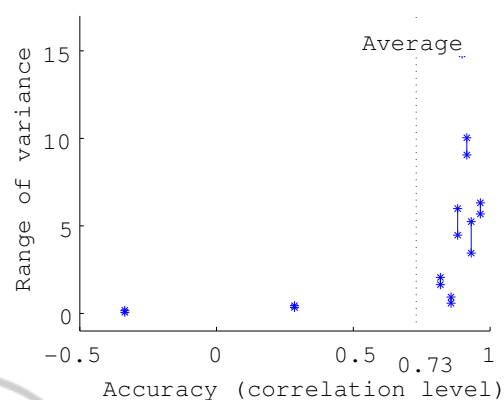


Figure 4: Accuracy of cADR vs the range of variance of cADR. This figure illustrates the relationship between the variance of cADR on the y axis and the correlation values between cADR and eADR on the x axis for data sets from 1 to 9. For each set of data, the maximum and minimum variance is denoted by '\*', and the range of variance is denoted by vertical lines. The accuracy (correlation level) for all images as a whole is 0.73.

scan path prediction. The computability of the distribution of 'idiosyncratic' scan path is confirmed. The feasibility of the computational prediction of scan paths is validated by eye movement experiment. It is suggested that the accuracy of the model can also be estimated by quantitative parameters explained in this study. The future direction would be to apply the scan path calculation to a longer sequence of fixations by finding the IPAs that is applicable to each temporal sequence of fixations.

## REFERENCES

- Bohme, M., Dorr, M., Krause, C., Martinetz, T., and Barth, E. (2004). Eye movement prediction of natural videos. *Neurocomputing*, Vol 69, 16-18, 1996-2004.
- Buswell, G. (1935). *How people look at pictures: A study of the psychology of perception in art*. University of Chicago Press, Chicago.
- Iiit, L., Koch, C., and Niebur, E. (1998). A model of saliency-based visual attention for rapid scene analysis. *IEEE Transactions on Pattern Analysis and Machine Intelligence* 20, 11, 1254-1259.
- Privitera, C. and Stark, L. (2000). Algorithms for defining visual regions-of-interest: Comparison with eye fixations. *IEEE Transactions of Pattern Analysis and Machine Intelligence*, Vol 22(9), 970-982.
- Robert, J., Jacob, K., and Karn, K. (2003). Eye tracking in human-computer interaction and usability research: ready to deliver promises. In *The Mind's Eye*. Elsevier Science BV.
- Tatler, B. (2007). The central fixation bias in scene viewing: selecting an optimal viewing position independently of motor biases and image feature distributions. *Journal of vision* 7(14):4, 1-7.